THE JOURNAL OF BIOLOGICAL CHEMISTRY VOL. 290, NO. 24, pp. 14841–14851, June 12, 2015

Maternal and Zygotic Sphingosine Kinase 2 Are Indispensable for Cardiac Development in Zebrafish*[S]

Received for publication, December 23, 2014, and in revised form, April 9, 2015 Published, JBC Papers in Press, April 23, 2015, DOI 10.1074/jbc.M114.634717

Yu Hisano[‡1], Asuka Inoue[§¶], Michiyo Okudaira[§], Kiyohito Taimatsu[‖], Hirotaka Matsumoto[§], Hirohito Kotani[‖], Rie Ohga[‖], Junken Aoki[§], and Atsuo Kawahara[‖2]**

*From the [‡]Laboratory for Developmental Gene Regulation, Brain Science Institute, RIKEN, 2-1 Hirosawa, Wako, Saitama 351-0198, the [§]Graduate School of Pharmaceutical Sciences, Tohoku University, 6-3 Aoba, Aramaki, Aoba-ku, Sendai, Miyagi 980-8578, [¶]PRESTO and **CREST, Japan Science and Technology Agency and [‖]Laboratory for Developmental Biology, Center for Medical Education and Sciences, Graduate School of Medical Science, University of Yamanashi, 1110 Shimokato, Chuo, Yamanashi 409-3898, Japan*

Background: Developmental functions of Sphk1 and Sphk2 remain unclear in vertebrates.
Results: Maternal-zygotic *sphk2* zebrafish mutant exhibited cardia bifida, whereas maternal-zygotic *sphk1*, maternal *sphk2*, and zygotic *sphk2* mutants did not.
Conclusion: Maternal and zygotic Sphk2 cooperatively regulate cardiac development.
Significance: The contribution of maternally supplied lipid mediators presents as a critical requirement for maternal-zygotic Sphk2 during cardiac development.

Sphingosine 1-phosphate (S1P) is synthesized from sphingosine by sphingosine kinases (SPHK1 and SPHK2) in invertebrates and vertebrates, whereas specific receptors for S1P (S1PRs) selectively appear in vertebrates, suggesting that S1P acquires novel functions in vertebrates. Because the developmental functions of SPHK1 and SPHK2 remain obscure in vertebrates, we generated *sphk1* or *sphk2* gene-disrupted zebrafish by introducing premature stop codons in their coding regions using transcription activator-like effector nucleases. Both zygotic *sphk1* and *sphk2* zebrafish mutants exhibited no obvious developmental defects and grew to adults. The maternal-zygotic *sphk2* mutant (*MZsphk2*), but not the maternal-zygotic *sphk1* mutant and maternal *sphk2* mutant, had a defect in the cardiac progenitor migration and a concomitant decrease in S1P level, leading to a two-heart phenotype (cardia bifida). Cardia bifida in *MZsphk2*, which was rescued by injecting *sphk2* mRNA, was a phenotype identical to that of zygotic mutants of the S1P transporter *spns2* and S1P receptor *s1pr2*, indicating that the Sphk2-Spns2-S1pr2 axis regulates the cardiac progenitor migration in zebrafish. The contribution of maternally supplied lipid mediators during vertebrate organogenesis presents as a requirement for maternal-zygotic Sphk2.

Sphingosine 1-phosphate (S1P)[3] is a bioactive lipid mediator that plays important roles in regulating crucial cellular processes, such as cell proliferation, migration, and differentiation (1, 2). S1P is intracellularly synthesized from sphingosine by sphingosine kinases (SPHK1 and SPHK2) and is released by S1P transporters, including SPNS2 (3, 4). The S1P released is recognized by G protein-coupled S1P receptors (S1PR1-S1PR5), leading to the activation of various downstream signaling pathways (5, 6). S1P also functions as an intracellular second messenger (7, 8). Conversely, various physiological roles, such as lymphocyte egress, vascular development, and bone homeostasis, are mediated by the intercellular S1P signaling pathway because these biological activities are affected in S1P receptors or transporter KO mice (9–12).

Both SPHK1 and SPHK2 contain conserved domains responsible for substrate binding and catalytic activity (13, 14). However, there are differences in cellular localization and substrate specificity (2, 6). Human SPHK1 is localized in the cytosol and translocated to the plasma membrane by various extracellular stimuli, whereas human SPHK2 localizes to the mitochondria, endoplasmic reticulum, and nucleus (5). Sphingosine and dihydro-sphingosine can be endogenous substrates of both SPHK1 and SPHK2. However, phyto-sphingosine and FTY720, which are sphingosine analogues, are preferentially catalyzed by SPHK2 (15–17); a phosphorylated form of FTY720 acts as an immunosuppressive agent through the S1PR1 receptor on mature lymphocytes (15, 16).

Sphk1 or *Sphk2* KO mice have been generated, and their loss-of-function phenotypes were analyzed to reveal the physiological roles of SPHKs. *Sphk1* or *Sphk2* single KO mice are viable and fertile; however, *Sphk1*/*2* double KO mice are embryonic lethal because of severe defects in the vascular and neural development (18, 19). Furthermore, $Sphk1^{-/-}Sphk2^{+/-}$ female mice are infertile due to defective decidualization, whereas *Sphk1* or *Sphk2* single KO female mice are normally fertile (20).

* This work was supported by the Japan Society for the Promotion of Science and the Program for Next Generation World-Leading Researchers (NEXT Program) and by Takeda Science Foundation. This work was also supported by the Special Postdoctoral Researcher Program (to Y. H.) from RIKEN and by PRESTO (Precursory Research for Embryonic Science and Technology; to A. I.) and CREST (to J. A.), from Japan Science and Technology Agency (JST).
[S] This article contains supplemental movies.
[1] To whom correspondence may be addressed. Tel.: 81-48-467-9713; Fax: 81-48-467-9714; E-mail: y.hisano@riken.jp.
[2] To whom correspondence may be addressed. Tel.: 81-55-273-9375; E-mail: akawahara@yamanashi.ac.jp.
[3] The abbreviations used are: S1P, sphingosine 1-phosphate; S1PR, S1P receptor; SPHK, sphingosine kinase; Sph, sphingosine; MO, morpholino oligomer; YSL, yolk syncytial layer; TALEN, transcription activator-like effector nuclease; dpf, days post-fertilization; LC-MS/MS, lipid chromatography-tandem mass spectrometry; GEF, guanine nucleotide exchange factor.

TABLE 1

Amino acid sequences of TALEN constructs

The repeat variable di-residue (RVD) sequences are indicated as red letters in the coding sequences of the indicated TALEN constructs.

sphk1-TALEN-F
MAPKKKRKVDYKDHDGDYKDHDIDYKDDDDKGTVDLRTLGYSQQQQEKIKPKVRSTVAQHHEALVGHGFT HAHIVALSQHPAALGTVAVTYQHIITALPEATHEDIVGVGKQWSGARALEALLTDAGELRGPPLQLDTGQ LVKIAKRGGVTAMEAVHASRNALTGAPLNLTPDQVVAIASNNGGKQALETVQRLLPVLCQDHGLTPDQVV AIASNNGGKQALETVQRLLPVLCQDHGLTPDQVVAIASNGGGKQALETVQRLLPVLCQDHGLTPDQVVAI ASNNGGKQALETVQRLLPVLCQDHGLTPDQVVAIASNIGGKQALETVQRLLPVLCQDHGLTPDQVVAIAS NIGGKQALETVQRLLPVLCQDHGLTPDQVVAIASHDGGKQALETVQRLLPVLCQDHGLTPDQVVAIASNN GGKQALETVQRLLPVLCQDHGLTPDQVVAIASNNGGKQALETVQRLLPVLCQDHGLTPDQVVAIASNNGG KQALETVQRLLPVLCQDHGLTPDQVVAIASHDGGKQALETVQRLLPVLCQDHGLTPDQVVAIASNGGGKQ ALETVQRLLPVLCQDHGLTPDQVVAIASNNGGKQALETVQRLLPVLCQDHGLTPDQVVAIASNIGGKQAL ETVQRLLPVLCQDHGLTPDQVVAIASNGGGKQALETVQRLLPVLCQDHGLTPDQVVAIASNNGGKQALET VQRLLPVLCQDHGLTPDQVVAIASNNGGKQALESIVAQLSRPDPALAALTNDHLVALACLGGRPAMDAVK KGLPHAPELIRRVNRRIGERTSHRVAGSQLVKSELEEKKSELRHKLKYVPHEYIELIEIARNSTQDRILE MKVMEFFMKVYGYRGKHLGGSRKPDGAIYTVGSPIDYGVIVDTKAYSGGYNLPIGQADEMQDYVEENQTR NKHINPNEWWKVYPSSVTEFKFLFVSGHFKGNYKAQLTRLNHITNCNGAVLSVEELLIGGEMIKAGTLTL EEVRRKFNNGEINF
sphk1-TALEN-R
MAPKKKRKVDYKDHDGDYKDHDIDYKDDDDKGTVDLRTLGYSQQQQEKIKPKVRSTVAQHHEALVGHGFT HAHIVALSQHPAALGTVAVTYQHIITALPEATHEDIVGVGKQWSGARALEALLTDAGELRGPPLQLDTGQ LVKIAKRGGVTAMEAVHASRNALTGAPLNLTPDQVVAIASHDGGKQALETVQRLLPVLCQDHGLTPDQVV AIASNGGGKQALETVQRLLPVLCQDHGLTPDQVVAIASNNGGKQALETVQRLLPVLCQDHGLTPDQVVAI ASNIGGKQALETVQRLLPVLCQDHGLTPDQVVAIASNIGGKQALETVQRLLPVLCQDHGLTPDQVVAIAS NGGGKQALETVQRLLPVLCQDHGLTPDQVVAIASNNGGKQALETVQRLLPVLCQDHGLTPDQVVAIASNN GGKQALETVQRLLPVLCQDHGLTPDQVVAIASHDGGKQALETVQRLLPVLCQDHGLTPDQVVAIASHDGG KQALETVQRLLPVLCQDHGLTPDQVVAIASNGGGKQALETVQRLLPVLCQDHGLTPDQVVAIASNGGGKQ ALETVQRLLPVLCQDHGLTPDQVVAIASHDGGKQALETVQRLLPVLCQDHGLTPDQVVAIASNGGGKQAL ETVQRLLPVLCQDHGLTPDQVVAIASHDGGKQALESIVAQLSRPDPALAALTNDHLVALACLGGRPAMDA VKKGLPHAPELIRRVNRRIGERTSHRVAGSQLVKSELEEKKSELRHKLKYVPHEYIELIEIARNSTQDRI LEMKVMEFFMKVYGYRGKHLGGSRKPDGAIYTVGSPIDYGVIVDTKAYSGGYNLPIGQAREMQRYVEENQ TRNKHINPNEWWKVYPSSVTEFKFLFVSGHFKGNYKAQLTRLNHITNCNGAVLSVEELLIGGEMIKAGTL TLEEVRRKFNNGEINF
sphk2-TALEN-F
MAPKKKRKVDYKDHDGDYKDHDIDYKDDDDKGTVDLRTLGYSQQQQEKIKPKVRSTVAQHHEALVGHGFT HAHIVALSQHPAALGTVAVTYQHIITALPEATHEDIVGVGKQWSGARALEALLTDAGELRGPPLQLDTGQ LVKIAKRGGVTAMEAVHASRNALTGAPLNLTPDQVVAIASHDGGKQALETVQRLLPVLCQDHGLTPDQVV AIASHDGGKQALETVQRLLPVLCQDHGLTPDQVVAIASNGGGKQALETVQRLLPVLCQDHGLTPDQVVAI ASNNGGKQALETVQRLLPVLCQDHGLTPDQVVAIASNGGGKQALETVQRLLPVLCQDHGLTPDQVVAIAS NNGGKQALETVQRLLPVLCQDHGLTPDQVVAIASNNGGKQALETVQRLLPVLCQDHGLTPDQVVAIASNN GGKQALETVQRLLPVLCQDHGLTPDQVVAIASNIGGKQALETVQRLLPVLCQDHGLTPDQVVAIASNIGG KQALETVQRLLPVLCQDHGLTPDQVVAIASNGGGKQALETVQRLLPVLCQDHGLTPDQVVAIASNGGGKQ ALETVQRLLPVLCQDHGLTPDQVVAIASHDGGKQALETVQRLLPVLCQDHGLTPDQVVAIASNGGGKQAL ETVQRLLPVLCQDHGLTPDQVVAIASNNGGKQALETVQRLLPVLCQDHGLTPDQVVAIASHDGGKQALET VQRLLPVLCQDHGLTPDQVVAIASHDGGKQALESIVAQLSRPDPALAALTNDHLVALACLGGRPAMDAVK KGLPHAPELIRRVNRRIGERTSHRVAGSQLVKSELEEKKSELRHKLKYVPHEYIELIEIARNSTQDRILE MKVMEFFMKVYGYRGKHLGGSRKPDGAIYTVGSPIDYGVIVDTKAYSGGYNLPIGQADEMQDYVEENQTR NKHINPNEWWKVYPSSVTEFKFLFVSGHFKGNYKAQLTRLNHITNCNGAVLSVEELLIGGEMIKAGTLTL EEVRRKFNNGEINF
sphk2-TALEN-R
MAPKKKRKVDYKDHDGDYKDHDIDYKDDDDKGTVDLRTLGYSQQQQEKIKPKVRSTVAQHHEALVGHGFT HAHIVALSQHPAALGTVAVTYQHIITALPEATHEDIVGVGKQWSGARALEALLTDAGELRGPPLQLDTGQ LVKIAKRGGVTAMEAVHASRNALTGAPLNLTPDQVVAIASNNGGKQALETVQRLLPVLCQDHGLTPDQVV AIASNIGGKQALETVQRLLPVLCQDHGLTPDQVVAIASNGGGKQALETVQRLLPVLCQDHGLTPDQVVAI ASNNGGKQALETVQRLLPVLCQDHGLTPDQVVAIASNNGGKQALETVQRLLPVLCQDHGLTPDQVVAIAS NIGGKQALETVQRLLPVLCQDHGLTPDQVVAIASNIGGKQALETVQRLLPVLCQDHGLTPDQVVAIASHD GGKQALETVQRLLPVLCQDHGLTPDQVVAIASHDGGKQALETVQRLLPVLCQDHGLTPDQVVAIASNIGG KQALETVQRLLPVLCQDHGLTPDQVVAIASNNGGKQALETVQRLLPVLCQDHGLTPDQVVAIASHDGGKQ ALETVQRLLPVLCQDHGLTPDQVVAIASNIGGKQALETVQRLLPVLCQDHGLTPDQVVAIASNIGGKQAL ETVQRLLPVLCQDHGLTPDQVVAIASNNGGKQALETVQRLLPVLCQDHGLTPDQVVAIASNGGGKQALET VQRLLPVLCQDHGLTPDQVVAIASNNGGKQALETVQRLLPVLCQDHGLTPDQVVAIASHDGGKQALETVQ RLLPVLCQDHGLTPDQVVAIASNIGGKQALESIVAQLSRPDPALAALTNDHLVALACLGGRPAMDAVKKG LPHAPELIRRVNRRIGERTSHRVAGSQLVKSELEEKKSELRHKLKYVPHEYIELIEIARNSTQDRILEMK VMEFFMKVYGYRGKHLGGSRKPDGAIYTVGSPIDYGVIVDTKAYSGGYNLPIGQAREMQRYVEENQTRNK HINPNEWWKVYPSSVTEFKFLFVSGHFKGNYKAQLTRLNHITNCNGAVLSVEELLIGGEMIKAGTLTLEE VRRKFNNGEINF

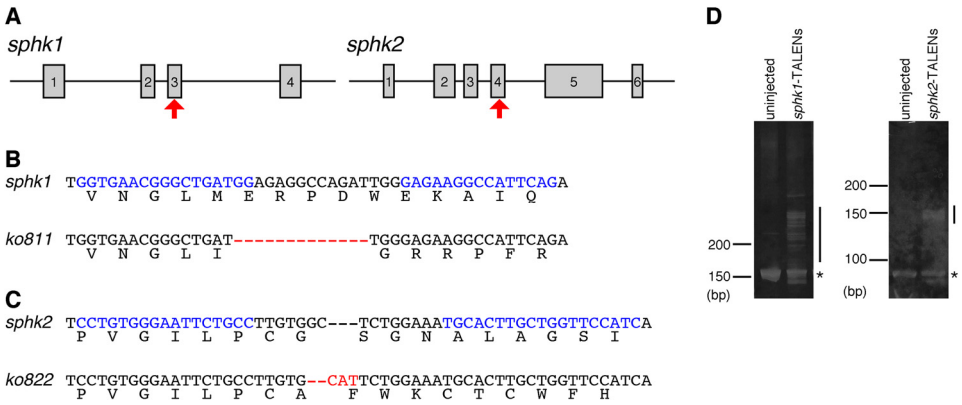

FIGURE 1. **Generation of *sphk1* and *sphk2* mutant zebrafish.** *A*, schematic representation of the *sphk1* and *sphk2* genes. Exons are shown as *gray boxes* with *numbers*. The TALEN-targeted genomic sites are indicated by *red arrows*. *B* and *C*, sequence alignment of the TALEN-generated alleles for *sphk1* (*B*) and *sphk2* (*C*). The 13 residues in *sphk1*^{ko811} indicated as *red bars* were deleted. Two residues in *sphk2*^{ko822} were deleted (*red bars*), and three residues were inserted (*red letters*). TALEN-recognizing sequences are indicated by *blue letters*. *D*, heteroduplex mobility assay to detect *sphk1* and *sphk2* TALEN-induced insertion and/or deletion mutations. Individual TALENs were injected into zebrafish embryos, and individual TALEN target regions were amplified from the genomic DNA of uninjected and TALEN-injected embryos. Individual PCR products were separated by 15% polyacrylamide gel electrophoresis. The expected homoduplex and multiple heteroduplex bands are indicated by *asterisks* and *lines*, respectively.

Taken together, SPHK1 and SPHK2 redundantly function during embryonic development.

S1P signaling is involved in cardiac and lower jaw development in zebrafish (11, 21, 22). Zygotic zebrafish mutants for *s1pr2* (S1P receptor) and *spns2* (S1P transporter) exhibit a defect in the cardiac progenitor migration, resulting in a two-heart phenotype known as cardia bifida (23–25). Furthermore, $G\alpha_{13}$/RhoGEF signaling has been identified downstream of S1pr2 in the endoderm (26); however, upstream molecules in this signaling pathway and the maternal contribution of S1P signaling remain obscure. Zebrafish is an ideal model organism to investigate the contribution of maternal factors, such as mRNAs, proteins, lipids, and nutrients, because zygotic gene expression begins around the 1,000-cell stage; thus, initial embryogenesis is regulated by maternal factors stored in blastomeres and yolk (27, 28). In clear contrast, zygotic expression starts in mice from the initial stage (two-cell stage), and proteins, lipids, and nutrients are supplied from the mother through the placenta (28). Thus, it is difficult to examine the contribution of maternal factors during early mammalian embryogenesis. Several mRNAs for S1P signaling-related molecules (*s1pr2*, *spp2*, and *sphk2*) are maternally supplied in zebrafish (29); however, their functions as maternal factors are not completely understood.

Recently, engineered nucleases, such as transcription activator-like effector nucleases (TALENs) and RNA-guided nucleases based on the type II bacterial clustered regularly interspaced short palindromic repeats (CRISPR)/CRISPR-associated (Cas) 9 system, have emerged and are useful in zebrafish (30, 31). These engineered nucleases induce DNA double-strand breaks in the targeted genomic locus, which could be repaired through an error-prone non-homologous end joining, leading to insertion and/or deletion mutations at the target site and to the frameshift-mediated gene disruption. To date, zebrafish is a valuable model vertebrate for maternal and/or zygotic mutant analyses, as they have both the forward and the reverse genetics.

In this study, we generated *sphk1* and *sphk2* mutant zebrafish using TALENs and analyzed the maternal and zygotic effects of *sphk1/2* during embryonic development.

Experimental Procedures

Zebrafish Mutants—Mutant alleles of *spns2*^{ko157} and *s1pr2*^{ko322} were used (21, 23, 32). *sphk1* and *sphk2* mutants were generated as described below.

Construction of TALEN Plasmids—The plasmids for synthesizing TALEN mRNAs were constructed in a two-step assembly system as described previously with some modifications (32, 33). Six or fewer TAL effector repeat modules were ligated into pFUS vectors (intermediate array vectors) as the first step (34). Subsequently, the intermediate array vectors and last TAL effector repeat were ligated into the pCS2TAL3DD vector for a forward TALEN or the pCS2TAL3RR vector for a reverse TALEN as the second step (35). The amino acid sequences of the constructed TALENs are shown in Table 1.

Preparation of mRNAs and Antisense Morpholino Oligomer—The plasmids for synthesizing TALEN, zebrafish *sphk2*, human *SPHK1*, or human *SPHK2* mRNA were linearized by NotI digestion, and mRNAs were transcribed using the mMESSAGE mMACHINE SP6 kit (Life Technologies) and purified using the RNeasy mini kit (Qiagen). Morpholino oligomer (MO) for *sphk2* (5′-AGCTCAAGTACATTTCATACCCAGC-3′) was purchased from Gene Tools.

Microinjection—Forward and reverse TALEN mRNAs (400 pg each) were injected together into the blastomeres of one-cell stage zebrafish embryos. MO and the synthesized mRNAs were dissolved in the injection buffer (40 mM HEPES (pH 7.4), 240 mM KCl, and 0.5% phenol red). The synthesized mRNA (1 pg) or MO (5 ng) was injected into one-cell stage zebrafish embryos or the yolk syncytial layer (YSL) around high stage embryos. Injection into the YSL was confirmed by the distribution of co-injected rhodamine-dextran (Sigma).

RNA Probes and Whole-mount in Situ Hybridization—RNA probes labeled with digoxigenin for *cmlc2*, *amhc*, *vmhc*, and *sphk2* were prepared using a RNA labeling kit (Roche Applied Science). Whole-mount *in situ* hybridization was performed as described previously (36).

FIGURE 2. **Amino acid sequence alignments of mammalian and zebrafish sphingosine kinases.** The ATP-binding domain and sphingosine (Sph)-binding domain are highlighted in *yellow* and *blue*, respectively. The frameshift-derived incorrectly translated amino acids are shown in *red*. *hSPHK1*, human SPHK1; *hSPHK2*, human SPHK2; *mSPHK1*, mouse SPHK1; *mSPHK2*, mouse SPHK2; *zSphk1*, zebrafish Sphk1; *zSphk2*, zebrafish Sphk2.

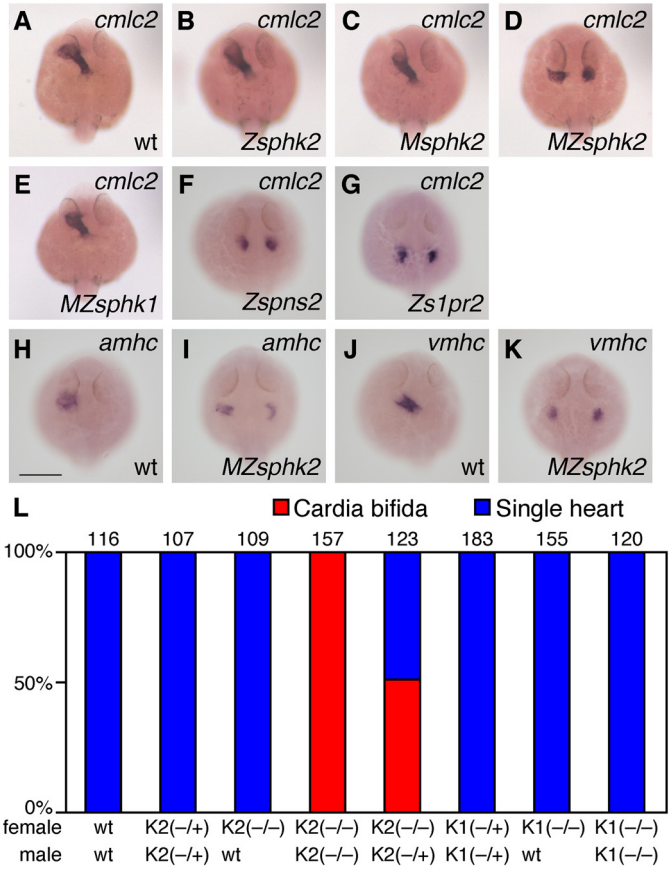

FIGURE 3. **Maternally and zygotically supplied *sphk2*, but not *sphk1*, is indispensable for cardiac progenitor migrations.** *A–G*, whole-mount *in situ* hybridization of *cmlc2*. Mating a homozygous *sphk2* (−/−) mutant female with a heterozygous (−/+) *sphk2* male produced 50% maternal-zygotic *sphk2* mutants (*MZsphk2*) and maternal *sphk2* mutants (*Msphk2*). Mating a heterozygous (−/+) *sphk2* female with a heterozygous (−/+) *sphk2* male produced 25% zygotic *sphk2* mutants (*Zsphk2*). The expression of *cmlc2* in wt embryos (*A*), *Zsphk2* mutants (*B*), *Msphk2* mutants (*C*), *MZsphk2* mutants (*D*), *MZsphk1* mutants (*E*), zygotic *spns2* (*Zspns2*) (*F*), and *s1pr2* (*Zs1pr2*) (*G*) at 24 h post-fertilization is shown. *H–K*, whole-mount *in situ* hybridization of the cardiac markers, atrial myosin heavy chain (*amhc*) and ventricular myosin heavy chain (*vmhc*). *L*, embryos exhibiting the two-heart phenotype, known as cardia bifida (*red*), or a normal single heart (*blue*) were quantified. The total number of embryos is shown at the *top* of each column. *K1*, *sphk1*; *K2*, *sphk2*. Mating was performed as indicated below the column (+, wild-type allele; −, mutant allele). *Scale bar*, 200 μm.

Genotyping of Mutant Alleles—Zebrafish embryos or fin clips were incubated in 50 μl of lysis buffer (10 mM Tris-HCl (pH 8.0), 1 mM EDTA, 0.2% Triton X-100, and 200 μg/ml proteinase K) at 55 °C for 3 h. Then, the solution was incubated at 100 °C for 10 min to inactivate the proteinase K. The TALEN target loci were amplified using the supernatants as templates and the following primers: Sphk1 forward, 5′-ACCTGTGTTTGTATGCGTGTGC-3′ and Sphk1 reverse, 5′-TGTGTCTGCTCACCGTGTGTAA-3′ for the *sphk1*-TALEN target locus; Sphk2 forward, 5′-GCCAGATTGGGAACAAGCAATA-3′ and Sphk2 reverse, 5′-CAGCATGGTGGTTGATGGAAC-3′ for the *sphk2*-TALEN target locus. PCR amplicons were electrophoresed on 15% polyacrylamide gels, and individuals were genotyped by heteroduplex mobility assay as described previously (37).

Alcian Blue Staining—Embryos were fixed at 3 days post-fertilization (dpf) in 4% paraformaldehyde in PBS and washed

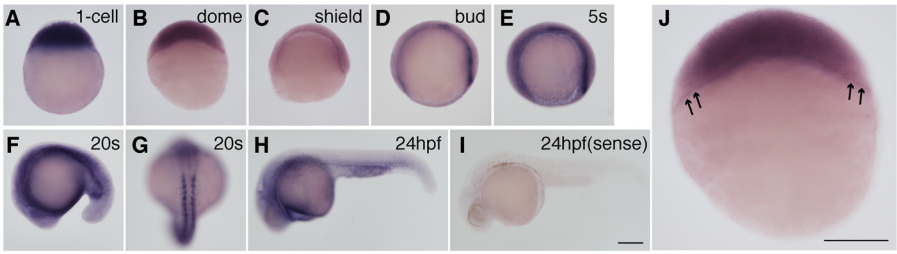

FIGURE 4. **Expression of *sphk2* during embryogenesis was examined by whole-mount *in situ* hybridization.** *A–J*, pictures present lateral views (*A–F* and *H–J*) and dorsal views (*G*): from the bud to the 20-somite stages presented anterior to the left (*D–F*, *H*, and *I*). *J*, magnified image of a dome stage embryo. *sphk2* transcripts were detected in the blastoderm and the YSL, as indicated by the *arrows*. *Scale bar*, 200 μm.

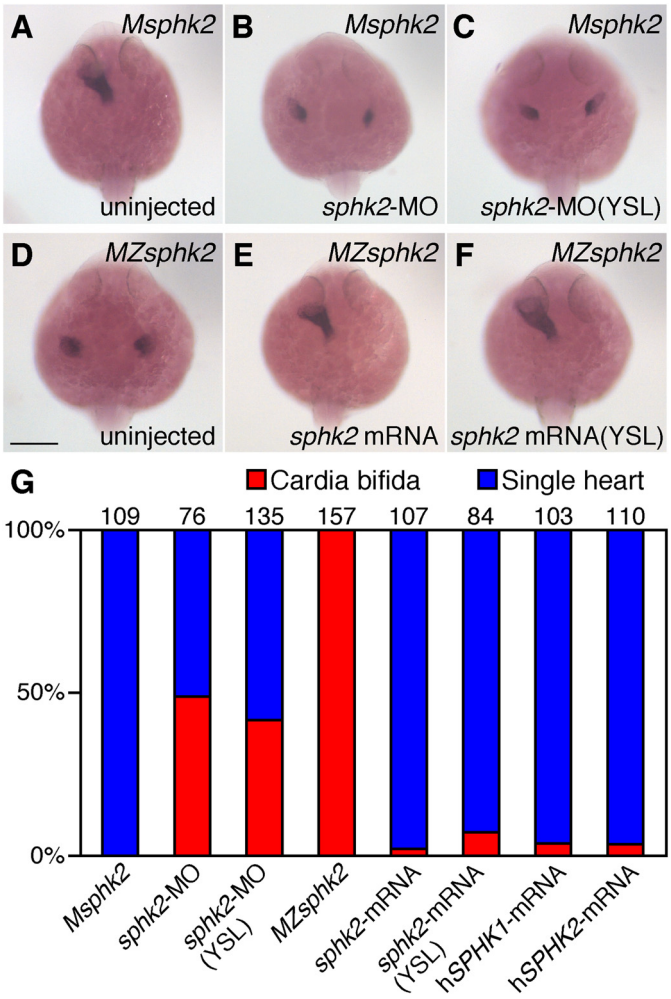

FIGURE 5. **sphk2 knockdown and rescue experiments.** *A–F*, whole-mount *in situ* hybridization of *cmlc2*. *A–C*, mating a homozygous *sphk2* (−/−) mutant female with a wild-type male produced 100% *Msphk2* mutants. *Msphk2* one-cell stage embryos were injected with *sphk2*-morpholino oligomer (5 ng) into the yolk at one-cell stage embryos (*B*) or into the YSL around high stage embryos as confirmed by the distribution of co-injected rhodaminedextran (*C*). *D–F*, *MZsphk2* embryos were injected with synthesized *sphk2* mRNA (1 pg) into the yolk at one-cell stage embryos (*E*) or into the YSL around high stage embryos as confirmed by the distribution of co-injected rhodaminedextran (*F*). *G*, embryos exhibiting cardia bifida (*red*) or a normal single heart (*blue*) were quantified. Human *SPHK1* or *SPHK2* mRNA was injected into *MZsphk2* embryos at the one-cell stage. The total number of embryos in each treatment is shown on the *top* of each column. *Scale bar*, 200 μm.

with acid alcohol buffer (0.37% HCl and 70% ethanol). After the incubation with 0.1% Alcian blue (Sigma) in acid alcohol buffer, the embryos were washed thrice with acid alcohol buffer.

Lysosphingolipid Analysis by Liquid Chromatography-Tandem Mass Spectrometry (LC-MS/MS)—Ten and five embryos were collected in a 1.5-ml siliconized tube at the two-cell stage and 5 dpf stage, respectively, and homogenized with a ultrasonic homogenizer (Smurt NR-50M, Microtech) in 200 μl of methanol in the presence of 1 μM dihydro-S1P (C17) as an internal standard. After further bath sonication for 10 min, the samples were centrifuged at 15,000 rpm for 10 min at 4 °C. The resulting supernatants were passed through a filter (0.22-μm pore size), and 10 μl of the filtrate was subjected to the LC-MS/MS analysis as described previously with some modifications (38, 39). LC separation was performed using a CAPCELL-PAK C18 ACR 1.5 × 100-mm column (Shiseido) with a gradient elution of solvent A (5 mM ammonium formate in water, pH 4.0) and solvent B (5 mM ammonium formate in 95% (v/v) acetonitrile, pH 4.0) at 250 μl/min. The initial conditions were set to 50% solvent B. The following solvent gradient was applied: maintain 50% solvent B for 0.2 min, followed by a linear gradient to 95% solvent B from 0.2 to 2.8 min, and hold at 95% solvent B for 2.2 min. Subsequently, the mobile phase was immediately returned to the initial conditions and maintained for 1.4 min. The ratio of an analyte peak area to the internal standard peak area was used for quantification. Lipid content was expressed as pmol per embryo.

Results

Generation of sphk1 and sphk2 Mutant Zebrafish—S1P is synthesized from sphingosine by SPHK1 and SPHK2. Because the developmental functions of SPHK1 and SPHK2 during vertebrate embryogenesis are not completely understood, we generated *sphk1* and *sphk2* gene-disrupted zebrafish using TALENs. The *sphk1* and *sphk2* TALENs were designed to target the third and fourth exons, respectively (Fig. 1*A*). Their *in vivo* activities of inducing insertion and/or deletion mutations at the targeted genomic loci were assessed by heteroduplex mobility assay (Fig. 1*D*). Individual TALEN-injected F0 founders were mated with wild-type zebrafish to establish the individual mutant lines. We identified the TALEN-mediated frameshift mutations in the $sphk1^{ko811}$ and $sphk2^{ko822}$ mutants: the $sphk1^{ko811}$ allele, with 13 deleted bases, composed of 74 correct amino acids from the start codon and 39 incorrect amino acids (Figs. 1*B* and 2), and the $sphk2^{ko822}$ allele, with two deleted bases and three inserted bases, composed of 257 correct amino acids from the start codon and 16 incorrect amino acids (Figs. 1*C* and 2). Characteristic domains, such as ATP-binding domain and sphingosine-binding domain, are present in mam-

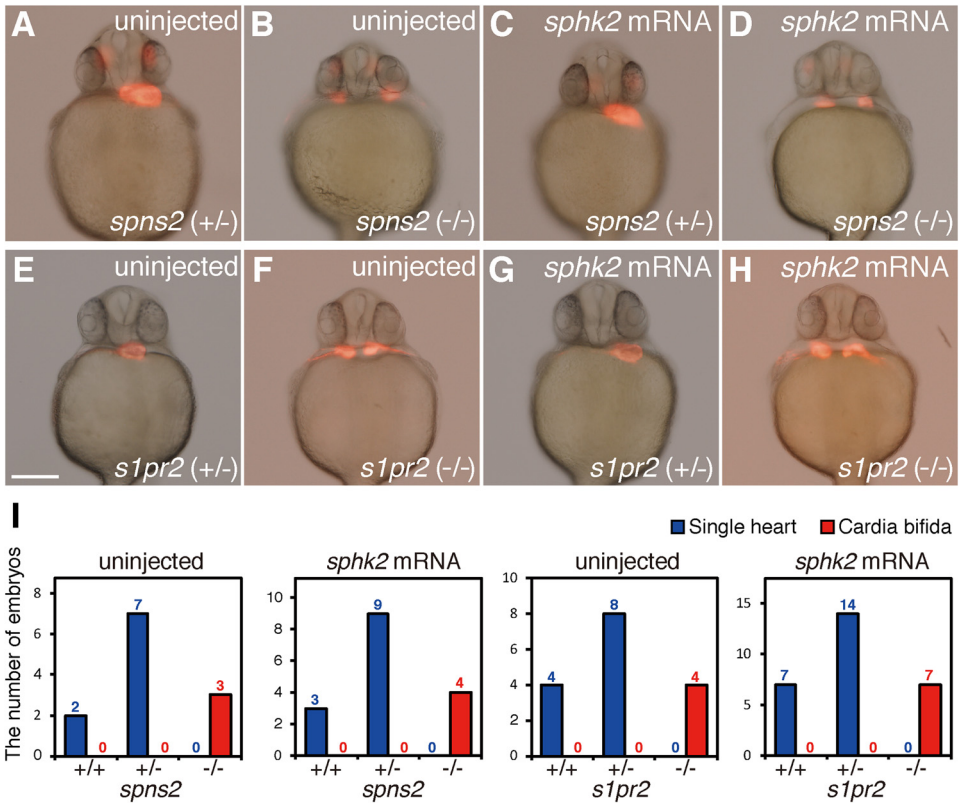

FIGURE 6. **sphk2 mRNA injection into zygotic *s1pr2* mutant or *spns2* mutant embryos.** *A–D*, embryos obtained from mating male and female *s1pr2* (−/+) were injected with synthesized *sphk2* mRNA (1 pg) into a blastomere at the one-cell stage. After taking pictures of phenotypic analysis, genomic DNAs were prepared from individual embryos, and genotyping of *s1pr2* mutant was determined by heteroduplex mobility assay. *E–H*, embryos obtained from mating male and female *spns2* (−/+) were injected with synthesized *sphk2* mRNA (1 pg) into a blastomere at the one-cell stage. After taking pictures of phenotypic analysis, genomic DNAs were prepared from individual embryos, and genotyping of *spns2* mutant was determined by direct sequence of *spns2* locus. *I*, embryos exhibiting cardia bifida (two-heart) or a normal single heart were quantified. The total number of embryos is shown on the *top* of each column. *Scale bar*, 200 μm.

malian SPHK1 and SPHK2, and both domains are conserved in zebrafish (13, 14). The 13-base deletion of the *sphk1*^{ko811} allele occurred inside the ATP-binding domain. Both the *sphk1*^{ko811} and the *sphk2*^{ko822} alleles lacked the sphingosine-binding domain (Fig. 2). Therefore, Sphk1^{ko811} and Sphk2^{ko822} were expected to lose their inherent S1P producing activities.

Maternal and Zygotic sphk2 Are Involved in Cardiac Progenitor Migration—We examined the zygotic *sphk1* and *sphk2* homozygous mutant phenotypes by crossing individual heterozygous males and females. Neither the zygotic *sphk1* nor the *sphk2* mutant exhibited any obvious developmental defects and grew to adults. Thereafter, we examined the developmental phenotypes of maternal and maternal-zygotic *sphk1* or *sphk2* gene mutants. As shown in Fig. 3, the maternal-zygotic *sphk2* mutant embryos (*MZsphk2*) exhibited cardia bifida-like zygotic *s1pr2* or *spns2* mutants, whereas the maternal *sphk2* mutant embryos (*Msphk2*) showed no obvious developmental defects similar to zygotic *sphk2* mutant. In clear contrast, the maternal-zygotic *sphk1* mutant embryos (*MZsphk1*) developed normally without cardia bifida and grew to adults (Fig. 3, *E* and *L*). Given that maternal and zygotic *sphk2*, but not maternal and zygotic *sphk1*, are required for cardiac development, we focused our study on the *sphk2* gene.

The expression of myocardial markers (*cmlc2*) and chamber-specific markers (*amhc* and *vmhc*) was detected in two separated domains (Fig. 3, *D*, *I*, and *K*). The separated hearts exhibited rhythmic beating (supplemental movies), suggesting that the cardiac progenitors differentiated into cardiomyocytes at bilateral positions.

sphk2 mRNA Expression during Embryogenesis—Whole-mount *in situ* hybridization analysis was performed to investigate *sphk2* expression patterns during embryogenesis (Fig. 4). *sphk2* expression was strongly detected at the one-cell stage (Fig. 4*A*), suggesting that *sphk2* mRNA is maternally supplied and consistent with a previous observation analyzed by quantitative real time PCR (29). Furthermore, *sphk2* transcripts in the YSL were detected from the dome stage to the 20-somite stage (Fig. 4, *B–F* and *J*). *sphk2* was transiently expressed in developing somites at the 20-somite stage (Fig. 4*G*).

Requirement of Zygotic sphk2 in the YSL during Cardiac Progenitor Migration—We knocked down zygotic *sphk2* by injecting a splice-blocking MO (*sphk2*-MO) into *Msphk2* embryos obtained from mating *sphk2*$^{ko822/ko822}$ females with wild-type males to delete maternal *sphk2* and confirm the requirement for zygotic *sphk2* during cardiac development (Fig. 5). When *sphk2*-MO was injected into *Msphk2* embryos at the one-cell stage, cardia bifida was observed (Fig. 5, *B* and *G*). *sphk2* expression in the YSL (Fig. 4) prompted us to perform a YSL-specific knockdown analysis. Cardia bifida was observed in *Msphk2* embryos injected with *sphk2*-MO into the YSL around high stage embryos (Fig. 5, *C* and *G*). These results were consistent with the finding that both maternally and zygotically supplied

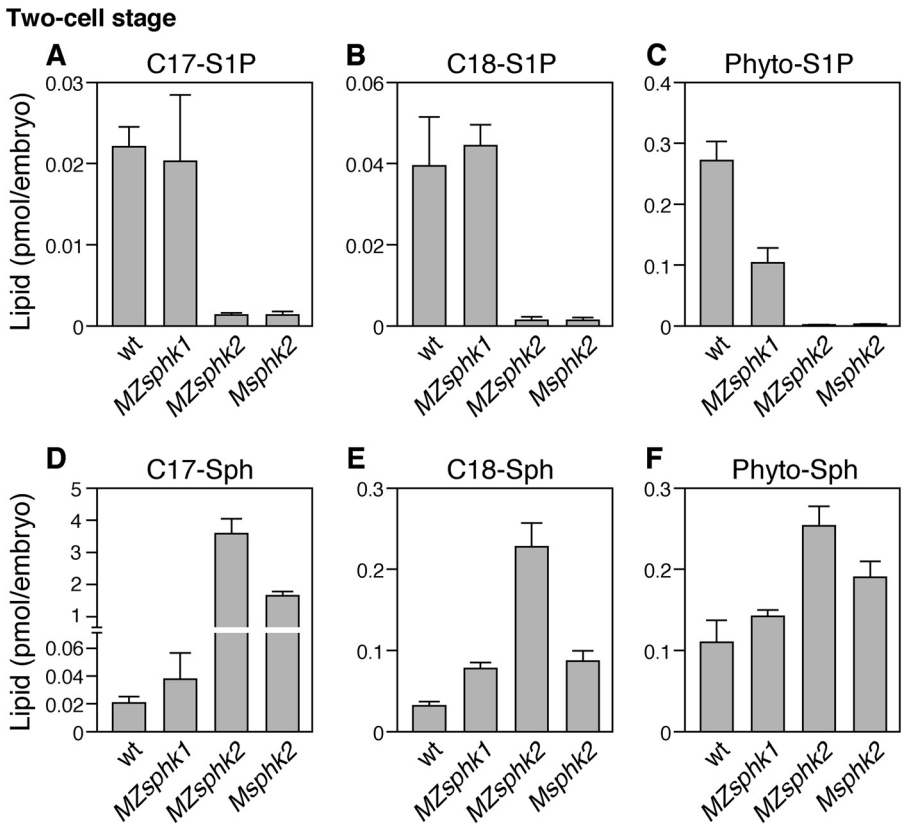

FIGURE 7. **Lysosphingolipid contents in fertilized eggs.** Two-cell stage embryos were collected from wt, *MZsphk1*, *MZsphk2*, and *Msphk2*. *A–F*, the quantities of C17-S1P (*A*), C18-S1P (*B*), phyto-S1P (*C*), C17-sphingosine (*C17-Sph*) (*D*), C18-sphingosine (*C18-Sph*) (*E*), and phyto-sphingosine (*Phyto-Sph*) (*F*) were quantified by liquid chromatography-tandem mass spectrometry. Bars and error bars represent means ± S.D., respectively, from five experiments.

sphk2 are involved in cardiac development, suggesting the importance of zygotically supplied *sphk2* mRNA in the YSL.

sphk mRNA Injection Rescues the MZsphk2 Cardiac Defect—We performed rescue experiments using synthetic *sphk2* mRNA to verify that the cardia bifida in *MZsphk2* embryos was caused by the *sphk2* gene mutation. Cardia bifida in *MZsphk2* embryos was rescued by the injecting *sphk2* mRNA at the one-cell stage embryos (Fig. 5, *E* and *G*). Furthermore, YSL-specific injection of *sphk2* mRNA rescued the cardiac defect (Fig. 5, *F* and *G*). These results suggest that injecting *sphk2* mRNA into the YSL is sufficient to produce the S1P required for migration of the cardiac progenitors. Injection of both human *SPHK2* mRNA and human *SPHK1* mRNA into one-cell stage *MZsphk2* embryos also rescued the cardiac defect (Fig. 5*G*), suggesting the importance of S1P production by sphingosine kinases in zebrafish cardiac development (Fig. 5*G*).

Sphk2 Is Genetically Located Upstream of the Spns2-S1pr2 Signaling—We examined whether zygotic *spns2* and *s1pr2* mutants were rescued or not by *sphk2* mRNA injection. Zebrafish *sphk2* mRNA was injected into one-cell stage embryos from heterozygous *spns2* or *s1pr2* mutants (23, 25). The cardia bifida phenotype in *spns2* or *s1pr2* mutants was not rescued by *sphk2* mRNA injection (Fig. 6), suggesting that Sphk2 acts upstream of Spns2 and S1pr2 in the cardiac development as expected by their molecular functions.

Lysosphingolipid Levels in Zebrafish Embryos—Two-cell stage embryos were collected to eliminate unfertilized eggs, and lysosphingolipid levels in the embryos were measured by LC-MS/MS. As shown in Fig. 7, about 0.02 pmol of C17-S1P, 0.04 pmol of C18-S1P, and 0.27 pmol of phyto-S1P exist in a fertilized wild-type egg. The quantities of these lysosphingolipid in *MZsphk2* were considerably lower when compared with those in the wild type, whereas precursors, such as C17-sphingosine, C18-sphingosine, and phyto-sphingosine, increased. In *Msphk2* embryos, the quantities of C17-S1P, C18-S1P, and phyto-S1P were also decreased to levels comparable with those in *MZsphk2*, whereas that of C18-sphingosine did not increase. Furthermore, the quantities of C17-S1P and C18-S1P remained unchanged in *MZsphk1*, whereas that of phyto-S1P decreased to 40% of that in the wild type, suggesting a functional requirement of *sphk1* for phyto-S1P production. These data suggest that the S1P accumulating in the two-cell stage embryos is mainly dependent on maternal *sphk2*.

Furthermore, sphingolipid levels at 5 dpf embryos were measured to examine the roles of zygotic sphingosine kinases. About 0.15 pmol of C17-S1P, 1 pmol of C18-S1P, and 0.4 pmol of phyto-S1P exist in a 5 dpf wild-type embryo (Fig. 8). The quantity of C17-S1P was decreased in *MZsphk1*. The quantities of C18-S1P and phyto-S1P were decreased in *MZsphk2* but not in *Msphk2*, suggesting that S1P synthesis at 5 dpf embryos was mainly dependent on zygotic *sphks*.

Tail Blister and Disorganized Jaw Phenotypes in MZsphk2—In addition to cardiac defect, both *s1pr2* and *spns2* mutants exhibited a tail blister phenotype that has not been observed in other characterized cardia bifida mutants (23–25). Cardia bifida and tail blister phenotypes were simultaneously exhib-

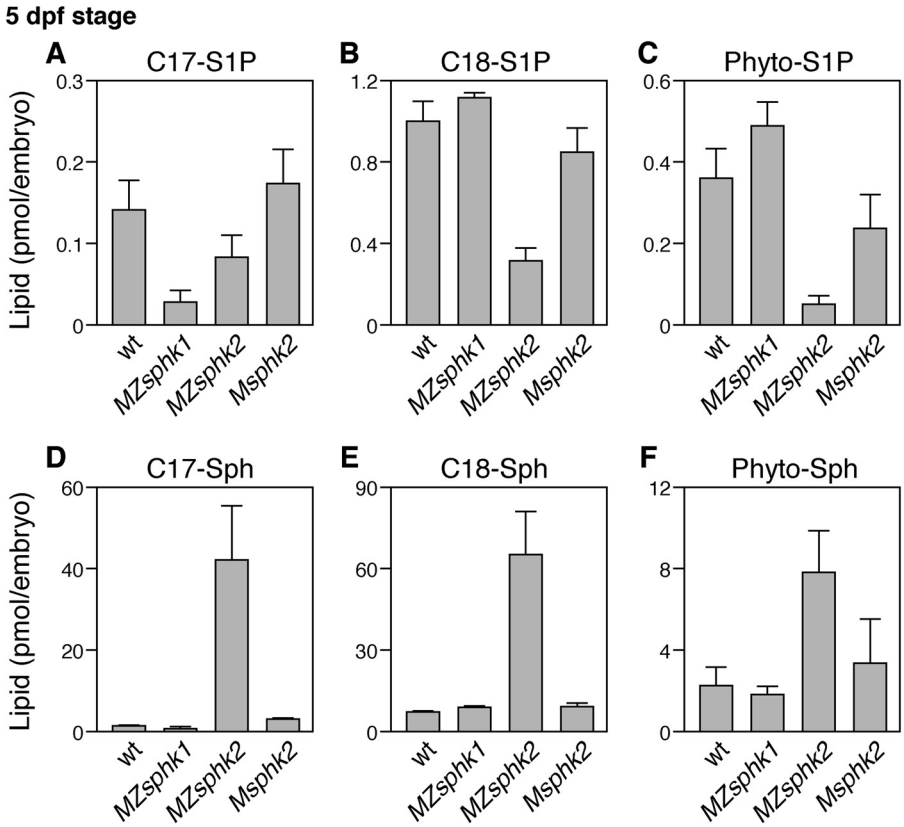

FIGURE 8. **Lysosphingolipid contents at 5 dpf embryos.** Embryos were collected from wt, *MZsphk1*, *MZsphk2*, and *Msphk2*. *A–F*, the quantities of C17-S1P (*A*), C18-S1P (*B*), phyto-S1P (*C*), C17-sphingosine (*C17-Sph*) (*D*), C18-sphingosine (*C18-Sph*) (*E*), and phyto-sphingosine (*Phyto-Sph*) (*F*) were quantified by liquid chromatography-tandem mass spectrometry. Bars and error bars represent means + S.D., respectively, from five experiments.

ited in about 25% of the progeny from a *spns2*$^{ko157/+}$ or *s1pr2*$^{ko322/+}$ incross, which is equivalent to a Mendelian ratio of a homozygous mutant (Fig. 9, *F*–H), suggesting that all zygotic *spns2* or *s1pr2* mutants are present as the tail blister phenotype. *MZsphk2* embryos, but not *MZsphk1*, *Msphk2*, or zygotic *sphk2* mutant embryos, exhibited tail blisters (Fig. 9), suggesting that both maternal and zygotic *sphk2* are also involved in fin morphology. However, unlike the *spns2* or *s1pr2* mutants, ~66% of *MZsphk2* embryos exhibited tail blisters, whereas cardia bifida was observed in all *MZsphk2* embryos (Figs. 3*L* and 9*H*).

Spns2-S1pr2 signaling also promotes the formation of the ventral pharyngeal cartilage, and zygotic *spns2* or *s1pr2* mutants exhibit lower jaw developmental defect (21, 22). We analyzed the pharyngeal arch structure of *MZsphk1* and *MZsphk2* embryos with Alcian blue staining. Lower jaw morphology was disorganized in *MZsphk2* embryos, but not in *MZsphk1* embryos (Fig. 10), indicating that Sphk2 produces the S1P required for lower jaw development.

Discussion

In this study, we present genetic evidence that both maternal and zygotic Sphk2 regulate the cardiac progenitor migration after analyzing *sphk* zebrafish mutants generated with TALENs. *Sphk1/2* double KO mice, but not *Sphk1* or *Sphk2* single KO mice, exhibited severe defects in the vascular and neural development (18, 19); however, the physiological roles specific to individual SPHKs remain unresolved. *MZsphk2* embryos, but not *MZsphk1* embryos, exhibited the impaired cardiac progenitor migration and disorganized tail and lower jaw morphologies, presenting the Sphk2-specific roles during early zebrafish embryogenesis. The tail blister phenotype was observed in ~66% of *MZsphk2* embryos (Fig. 9*H*), whereas the homozygous *spns2* or *s1pr2* mutant simultaneously exhibited cardia bifida and tail blister phenotypes, and all *MZsphk2* exhibited cardia bifida, suggesting an auxiliary role for Sphk1 in fin morphogenesis. Unlike *MZsphk2*, *MZsphk1* fish were viable and fertile without any apparent developmental defects. Sphk1 may play physiological roles during later developmental stages cooperatively with Sphk2. We may have observed Sphk1-specific phenotypes when we performed some stress tests or perturbations. There are possibilities that the zebrafish genome may have other *sphks* from genome duplication and that S1P could be produced by an uncharacterized Sphk-independent pathway(s).

Previous studies have shown that S1P signaling through Spns2 and S1pr2 regulates the cardiac progenitor migration (23–25). Although *s1pr2* transcripts were detected in the endoderm and cardiac progenitors, $G\alpha_{13}$/RhoGEF activation in the endoderm downstream of S1pr2 is essential for cardiac progenitor migration (26). *spns2* transcripts were expressed in the YSL, which is a transient extra-embryonic syncytial tissue formed by ventrally located blastomeres around the 1,000-cell stage. Subsequently, the yolk and blastoderm are physically separated by the YSL, and yolk contents (mRNAs, proteins, etc.) cannot easily diffuse into the blastoderm after the YSL formation (40). We

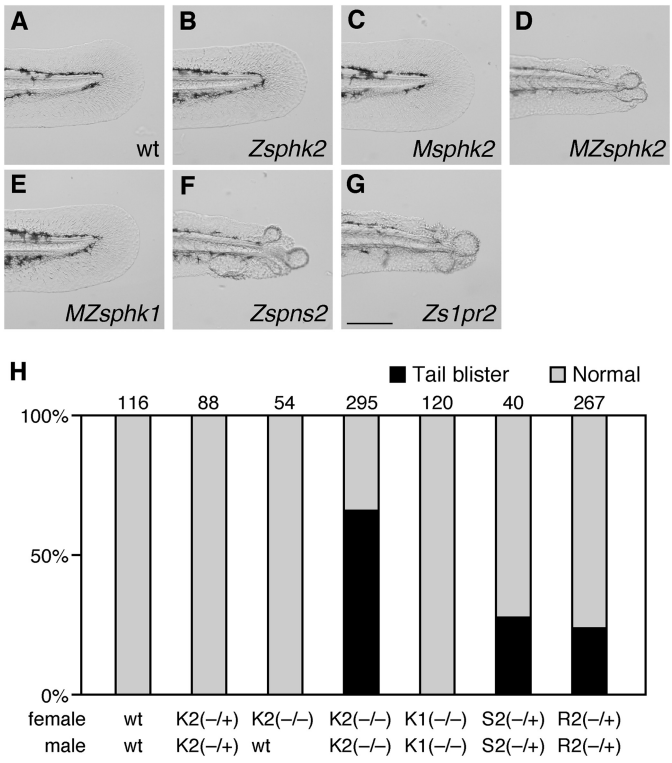

FIGURE 9. **MZsphk2 embryos exhibit the tail blister phenotype.** *A–G*, lateral bright field images of the medial fin at 2 dpf embryos. *MZsphk2*, zygotic *spns2* (*Zspns2*), and zygotic *s1pr2* (*Zs1pr2*) embryos show the tail blister phenotype, whereas wt, *MZsphk1*, zygotic *sphk2* (*Zsphk2*), and *Msphk2* embryos show normal fins. *H*, embryos exhibiting the tail blister (*black*) or normal fin (gray) phenotypes were quantified. The total number of embryos is shown on the *top* of each column. *K1*, *sphk1*; *K2*, *sphk2*; *S2*, *spns2*; *R2*, *s1pr2*. Mating was performed as indicated below the column (+, wild-type allele; −, mutant allele). *Scale bar*, 200 μm.

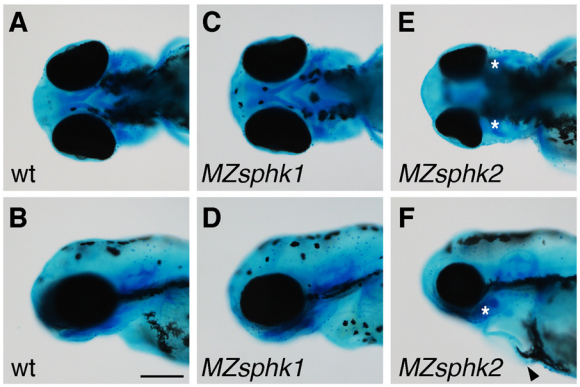

FIGURE 10. **Lower jaw morphology.** *A–F*, lower jaw morphology of wt (*A* and *B*), *MZsphk1* (*C* and *D*), and *MZsphk2* embryos (*E* and *F*) at 3 dpf was visualized with Alcian blue staining (*A*, *C*, and *E*, ventral view; *B*, *D*, and *F*, lateral view). The ventral pharyngeal arches of *MZsphk2*, but not *MZsphk1* embryos, were disorganized; vestiges are shown as *asterisks*. Cardiac edema was also observed in *MZsphk2* embryos, as shown by the *black arrowhead* (*F*). *Scale bar*, 200 μm.

found that YSL-specific knockdown of *spns2* by *spns2*-specific MO induced cardia bifida (23), suggesting that Spns2 supplies the S1P from the YSL to S1pr2 in the endoderm, resulting in the activation of $G\alpha_{13}$/RhoGEF to regulate cardiac progenitor migration. In this study, we demonstrated that *sphk2* required for cardiac progenitor migration is supplied maternally and zygotically, whereas the loss of zygotically supplied *s1pr2* or *spns2* induced cardia bifida. Zygotic *sphk2* mutant did not exhibit cardia bifida, probably because maternally supplied S1P is accumulated in the yolk and can recover the loss of S1P derived from zygotic *sphk2*. Conversely, the depletion of maternally derived S1P could have been recovered by *sphk2* expressed in the YSL during cardiac development.

Fertilized eggs contain significant quantities of S1P (Fig. 7, *A* and *B*), which dramatically decreased in *MZsphk2* and *Msphk2* embryos, suggesting that most of the S1P is not produced by zygotic Sphk2 but by maternal Sphk2 at the two-cell stage. At the 5 dpf stage, however, quantity of the abundant S1P species, C18-S1P, is reduced in *MZsphk2* embryos, but almost unchanged in *Msphk2* or *MZsphk1* embryos (Fig. 8*B*), showing that zygotic Sphk2 is a major S1P supplier at this stage. The reduced S1P level was reflected in concomitant accumulation of a metabolic precursor, sphingosine (Fig. 8*E*). Thus, the biochemical data clearly demonstrate that both maternal Sphk2 and zygotic Sphk2 can supply S1P in embryos (or fertilized eggs), which is consistent with the genetic evidence that both maternal and zygotic *sphk2* are required for the cardiac progenitor migration.

We detected *sphk2* transcripts in the YSL at the dome stage (Fig. 4*J*), and YSL-specific knockdown of *sphk2* in *Msphk2* embryos induced cardia bifida (Fig. 5*C*), suggesting that some of the zygotically supplied *sphk2* was located in the YSL to produce S1P, which can be efficiently transported by Spns2. In addition, injecting not only human *SPHK2* but also human *SPHK1* mRNA rescued the cardiac defect of *MZsphk2* (Fig. 5*G*), suggesting that human SPHK1 and SPHK2 have an ability to phosphorylate sphingosine in zebrafish and that the resultant increase in S1P level activated the signaling pathway essential for the cardiac progenitor migration in the *MZsphk2* mutant.

LC-MS/MS analysis revealed that the depletion of maternal *sphk2* caused the decrease in C17-S1P and a considerable increase in its precursor, C17-sphingosine (Fig. 7, *A* and *D*). Although the quantity of C18-S1P also decreased in *MZsphk2* and *Msphk2* embryos, that of C18-sphingosine, a precursor of C18-S1P, increased to a lesser degree in *MZsphk2* embryos, but not in *Msphk2* embryos at two-cell stage (Fig. 7, *B* and *E*). We speculate that the metabolic pathways between C17- and C18-sphingosine may be different in zebrafish or that C18-sphingosine may be degraded to biosynthesize other lipids. In mammals, phyto-sphingosine is phosphorylated by SPHK2, but not by SPHK1 (17). However, unlike C17- and C18-S1P, the quantity of phyto-S1P decreased 60% in *MZsphk1* at two-cell stage, suggesting that zebrafish Sphk1 is involved in phyto-S1P production. Therefore, endogenous substrates of Sphk1/2 may be slightly different between mammals and zebrafish. Phyto-sphingosine and phyto-S1P are predominant in plants and fungi and exist only in certain tissues, including the skin, small intestine, and kidney in mammals (2). In zebrafish-fertilized eggs, phyto-S1P was stored at about a 10-fold higher concentration than S1P (Fig. 7, *A* and *C*), although phyto-S1P levels became lower than C18-S1P at 5 dpf (Fig. 8, *A* and *C*), suggesting that phyto-S1P, in addition to S1P, may play physiological roles during zebrafish early embryogenesis.

Loss-of-function analyses of S1PRs in mice revealed that S1PR-mediated signaling is involved in physiological events, such as lymphocyte egress, angiogenesis, and bone homeosta-

sis. In addition, it has been proposed that S1P functions as a second messenger in the intracellular compartment. In mammals, tumor necrosis factor receptor-associated factor 2 and histone deacetylases have been identified as intracellular S1P targets (7, 8). Recently, it was reported that SPHK2-derived S1P in megakaryocytes controls the expression of Src family kinases and is not mediated by the S1P receptor (41). We found that cardia bifida, tail blister, and disorganized jaw morphology phenotypes observed in *MZsphk2* were identical to those observed in zygotic *spns2* or *s1pr2* mutants (21–25), suggesting that Sphk2-derived S1P functions as an intercellular signaling molecule and that the Sphk2-Spns2-S1pr2 signaling axis plays essential roles during cardiac and lower jaw development. In addition to S1P, dihydro-S1P, which is produced by SPHKs, can be an endogenous ligand for S1P receptors (42, 43), raising the possibility that this signaling pathway might be through dihydro-S1P.

In summary, we revealed that Sphk2, but not Sphk1, acts as an upstream molecule in the Spns2-mediated intercellular S1P signaling pathway, regulating cardiac progenitor migration, suggesting that Sphk2-derived S1P in the YSL is upstream of the Spns2-S1pr2 axis.

Acknowledgment—We thank Hitoshi Okamoto for support and for providing the opportunity to conduct this work.

Note Added in Proof—The supplemental movies were missing from the version of this article that was published as a Paper in Press on April 23, 2015. The movies are now available.

References

1. Neubauer, H. A., and Pitson, S. M. (2013) Roles, regulation and inhibitors of sphingosine kinase 2. *FEBS J.* **280,** 5317–5336
2. Kihara, A., Mitsutake, S., Mizutani, Y., and Igarashi, Y. (2007) Metabolism and biological functions of two phosphorylated sphingolipids, sphingosine 1-phosphate and ceramide 1-phosphate. *Prog. Lipid Res.* **46,** 126–144
3. Hannun, Y. A., and Obeid, L. M. (2008) Principles of bioactive lipid signalling: lessons from sphingolipids. *Nat. Rev. Mol. Cell Biol.* **9,** 139–150
4. Hisano, Y., Kobayashi, N., Kawahara, A., Yamaguchi, A., and Nishi, T. (2011) The sphingosine 1-phosphate transporter, SPNS2, functions as a transporter of the phosphorylated form of the immunomodulating agent FTY720. *J. Biol. Chem.* **286,** 1758–1766
5. Orr Gandy, K. A., and Obeid, L. M. (2013) Targeting the sphingosine kinase/sphingosine 1-phosphate pathway in disease: review of sphingosine kinase inhibitors. *Biochim. Biophys. Acta* **1831,** 157–166
6. Strub, G. M., Maceyka, M., Hait, N. C., Milstien, S., and Spiegel, S. (2010) Extracellular and intracellular actions of sphingosine-1-phosphate. *Adv. Exp. Med. Biol.* **688,** 141–155
7. Alvarez, S. E., Harikumar, K. B., Hait, N. C., Allegood, J., Strub, G. M., Kim, E. Y., Maceyka, M., Jiang, H., Luo, C., Kordula, T., Milstien, S., and Spiegel, S. (2010) Sphingosine-1-phosphate is a missing cofactor for the E3 ubiquitin ligase TRAF2. *Nature* **465,** 1084–1088
8. Hait, N. C., Allegood, J., Maceyka, M., Strub, G. M., Harikumar, K. B., Singh, S. K., Luo, C., Marmorstein, R., Kordula, T., Milstien, S., and Spiegel, S. (2009) Regulation of histone acetylation in the nucleus by sphingosine-1-phosphate. *Science* **325,** 1254–1257
9. Nishi, T., Kobayashi, N., Hisano, Y., Kawahara, A., and Yamaguchi, A. (2014) Molecular and physiological functions of sphingosine 1-phosphate transporters. *Biochim. Biophys. Acta* **1841,** 759–765
10. Obinata, H., and Hla, T. (2012) Sphingosine 1-phosphate in coagulation and inflammation. *Semin. Immunopathol.* **34,** 73–91
11. Hisano, Y., Nishi, T., and Kawahara, A. (2012) The functional roles of S1P in immunity. *J. Biochem.* **152,** 305–311
12. Hisano, Y., Kobayashi, N., Yamaguchi, A., and Nishi, T. (2012) Mouse SPNS2 functions as a sphingosine-1-phosphate transporter in vascular endothelial cells. *PLoS One* **7,** e38941
13. Pitson, S. M., Moretti, P. A., Zebol, J. R., Zareie, R., Derian, C. K., Darrow, A. L., Qi, J., D'Andrea, R. J., Bagley, C. J., Vadas, M. A., and Wattenberg, B. W. (2002) The nucleotide-binding site of human sphingosine kinase 1. *J. Biol. Chem.* **277,** 49545–49553
14. Yokota, S., Taniguchi, Y., Kihara, A., Mitsutake, S., and Igarashi, Y. (2004) Asp177 in C4 domain of mouse sphingosine kinase 1a is important for the sphingosine recognition. *FEBS Lett.* **578,** 106–110
15. Brinkmann, V., Billich, A., Baumruker, T., Heining, P., Schmouder, R., Francis, G., Aradhye, S., and Burtin, P. (2010) Fingolimod (FTY720): discovery and development of an oral drug to treat multiple sclerosis. *Nat. Rev. Drug. Discov.* **9,** 883–897
16. Kihara, A., and Igarashi, Y. (2008) Production and release of sphingosine 1-phosphate and the phosphorylated form of the immunomodulator FTY720. *Biochim. Biophys. Acta* **1781,** 496–502
17. Liu, H., Sugiura, M., Nava, V. E., Edsall, L. C., Kono, K., Poulton, S., Milstien, S., Kohama, T., and Spiegel, S. (2000) Molecular cloning and functional characterization of a novel mammalian sphingosine kinase type 2 isoform. *J. Biol. Chem.* **275,** 19513–19520
18. Allende, M. L., Sasaki, T., Kawai, H., Olivera, A., Mi, Y., van Echten-Deckert, G., Hajdu, R., Rosenbach, M., Keohane, C. A., Mandala, S., Spiegel, S., and Proia, R. L. (2004) Mice deficient in sphingosine kinase 1 are rendered lymphopenic by FTY720. *J. Biol. Chem.* **279,** 52487–52492
19. Mizugishi, K., Yamashita, T., Olivera, A., Miller, G. F., Spiegel, S., and Proia, R. L. (2005) Essential role for sphingosine kinases in neural and vascular development. *Mol. Cell Biol.* **25,** 11113–11121
20. Mizugishi, K., Li, C., Olivera, A., Bielawski, J., Bielawska, A., Deng, C. X., and Proia, R. L. (2007) Maternal disturbance in activated sphingolipid metabolism causes pregnancy loss in mice. *J. Clin. Invest.* **117,** 2993–3006
21. Hisano, Y., Ota, S., Takada, S., and Kawahara, A. (2013) Functional cooperation of *spns2* and *fibronectin* in cardiac and lower jaw development. *Biol. Open* **2,** 789–794
22. Balczerski, B., Matsutani, M., Castillo, P., Osborne, N., Stainier, D. Y. R., and Crump, J. G. (2012) Analysis of sphingosine-1-phosphate signaling mutants reveals endodermal requirements for the growth but not dorsoventral patterning of jaw skeletal precursors. *Dev. Biol.* **362,** 230–241
23. Kawahara, A., Nishi, T., Hisano, Y., Fukui, H., Yamaguchi, A., and Mochizuki, N. (2009) The sphingolipid transporter Spns2 functions in migration of zebrafish myocardial precursors. *Science* **323,** 524–527
24. Osborne, N., Brand-Arzamendi, K., Ober, E. A., Jin, S.-W., Verkade, H., Holtzman, N. G., Yelon, D., and Stainier, D. Y. R. (2008) The Spinster homolog, Two of Hearts, is required for sphingosine 1-phosphate signaling in zebrafish. *Curr. Biol.* **18,** 1882–1888
25. Kupperman, E., An, S., Osborne, N., Waldron, S., and Stainier, D. Y. (2000) A sphingosine-1-phosphate receptor regulates cell migration during vertebrate heart development. *Nature* **406,** 192–195
26. Ye, D., and Lin, F. (2013) S1pr2/Gα_{13} signaling controls myocardial migration by regulating endoderm convergence. *Development* **140,** 789–799
27. Langdon, Y. G., and Mullins, M. C. (2011) Maternal and zygotic control of zebrafish dorsoventral axial patterning. *Annu. Rev. Genet.* **45,** 357–377
28. Li, L., Zheng, P., and Dean, J. (2010) Maternal control of early mouse development. *Development* **137,** 859–870
29. Mendelson, K., Zygmunt, T., Torres-Vázquez, J., Evans, T., and Hla, T. (2013) Sphingosine 1-phosphate receptor signaling regulates proper embryonic vascular patterning. *J. Biol. Chem.* **288,** 2143–2156
30. Kim, H., and Kim, J. S. (2014) A guide to genome engineering with programmable nucleases. *Nat. Rev. Genet.* **15,** 321–334
31. Hisano, Y., Ota, S., and Kawahara, A. (2014) Genome editing using artificial site-specific nucleases in zebrafish. *Dev. Growth Differ.* **56,** 26–33
32. Hisano, Y., Ota, S., Arakawa, K., Muraki, M., Kono, N., Oshita, K., Sakuma, T., Tomita, M., Yamamoto, T., Okada, Y., and Kawahara, A. (2013) Quantitative assay for TALEN activity at endogenous genomic loci. *Biol. Open* **2,** 363–367
33. Cermak, T., Doyle, E. L., Christian, M., Wang, L., Zhang, Y., Schmidt, C., Baller, J. A., Somia, N. V., Bogdanove, A. J., and Voytas, D. F. (2011) Effi-

cient design and assembly of custom TALEN and other TAL effector-based constructs for DNA targeting. *Nucleic Acids Res.* **39,** e82
34. Sakuma, T., Hosoi, S., Woltjen, K., Suzuki, K., Kashiwagi, K., Wada, H., Ochiai, H., Miyamoto, T., Kawai, N., Sasakura, Y., Matsuura, S., Okada, Y., Kawahara, A., Hayashi, S., and Yamamoto, T. (2013) Efficient TALEN construction and evaluation methods for human cell and animal applications. *Genes. Cells* **18,** 315–326
35. Dahlem, T. J., Hoshijima, K., Jurynec, M. J., Gunther, D., Starker, C. G., Locke, A. S., Weis, A. M., Voytas, D. F., and Grunwald, D. J. (2012) Simple methods for generating and detecting locus-specific mutations induced with TALENs in the zebrafish genome. *PLoS Genet.* **8,** e1002861
36. Hanaoka, R., Katayama, S., Dawid, I. B., and Kawahara, A. (2006) Characterization of the heme synthesis enzyme coproporphyrinogen oxidase (CPO) in zebrafish erythrogenesis. *Genes Cells* **11,** 293–303
37. Ota, S., Hisano, Y., Muraki, M., Hoshijima, K., Dahlem, T. J., Grunwald, D. J., Okada, Y., and Kawahara, A. (2013) Efficient identification of TALEN-mediated genome modifications using heteroduplex mobility assays. *Genes Cells* **18,** 450–458
38. Saigusa, D., Shiba, K., Inoue, A., Hama, K., Okutani, M., Iida, N., Saito, M., Suzuki, K., Kaneko, T., Suzuki, N., Yamaguchi, H., Mano, N., Goto, J., Hishinuma, T., Aoki, J., and Tomioka, Y. (2012) Simultaneous quantitation of sphingoid bases and their phosphates in biological samples by liquid chromatography/electrospray ionization tandem mass spectrometry. *Anal. Bioanal. Chem.* **403,** 1897–1905
39. Okudaira, M., Inoue, A., Shuto, A., Nakanaga, K., Kano, K., Makide, K., Saigusa, D., Tomioka, Y., and Aoki, J. (2014) Separation and quantification of 2-acyl-1-lysophospholipids and 1-acyl-2-lysophospholipids in biological samples by LC-MS/MS. *J. Lipid Res.* **55,** 2178–2192
40. Carvalho, L., and Heisenberg, C. P. (2010) The yolk syncytial layer in early zebrafish development. *Trends Cell Biol.* **20,** 586–592
41. Zhang, L., Urtz, N., Gaertner, F., Legate, K. R., Petzold, T., Lorenz, M., Mazharian, A., Watson, S. P., and Massberg, S. (2013) Sphingosine kinase 2 (Sphk2) regulates platelet biogenesis by providing intracellular sphingosine 1-phosphate (S1P). *Blood* **122,** 791–802
42. Spiegel, S., and Milstien, S. (2000) Functions of a new family of sphingosine-1-phosphate receptors. *Biochim. Biophys. Acta* **1484,** 107–116
43. Kimura, T., Watanabe, T., Sato, K., Kon, J., Tomura, H., Tamama, K., Kuwabara, A., Kanda, T., Kobayashi, I., Ohta, H., Ui, M., and Okajima, F. (2000) Sphingosine 1-phosphate stimulates proliferation and migration of human endothelial cells possibly through the lipid receptors, Edg-1 and Edg-3. *Biochem. J.* **348,** 71–76